Soil moisture as a potential variable for tracking and quantifying irrigation: A case study with proximal gamma-ray spectroscopy data

Paolo Filippucci [a,*], Angelica Tarpanelli [a], Christian Massari [a], Andrea Serafini [b,c], Virginia Strati [b,c], Matteo Alberi [b,d], Kassandra Giulia Cristina Raptis [b,d], Fabio Mantovani [b,c], Luca Brocca [a]

[a] Research Institute for Geo-Hydrological Protection, National Research Council, Perugia, Italy
[b] Department of Physics and Earth Sciences, University of Ferrara, Via Saragat 1, 44121, Ferrara, Italy
[c] National Institute for Nuclear Physics, Ferrara Section, Via Saragat 1, 44121, Ferrara, Italy
[d] National Institute for Nuclear Physics, Legnaro National Laboratories, Viale dell'Università 2, 35020, Legnaro, Italy

A R T I C L E I N F O

A B S T R A C T

The global warming effects put in danger global water availability and make necessary to decrease water wastage, e.g., by monitoring global irrigation. Despite this, global irrigation information is scarce due to the absence of a solid estimation technique. In this study, we applied an innovative approach to retrieve irrigation water from high spatial and temporal resolution Soil Moisture (SM) data obtained from an advanced sensor based on Proximal Gamma-Ray (PGR) spectroscopy, in a field located in Emilia Romagna (Italy).

The results show that SM is a key variable to obtain information about the amount of water applied to plants, with Pearson correlation between observed and estimated daily irrigation data ranges from 0.88 to 0.91 by using different calibration methodology. With the aim of reproducing the working conditions of satellites measuring soil moisture, we sub-sampled SM hourly time series at larger time steps. The results demonstrated that the methodology is still capable to perform the daily (weekly) irrigation estimation with Pearson Correlation around 0.6 (0.7) if the time step is not greater than 36 (48) hours.

1. Introduction

Irrigation is one of the greatest human intervention on water cycle and it accounts for more than 70% of global freshwater withdrawals (FAO, 2006; Foley et al., 2011). Nowadays, around 20% of the world's cultivated area is irrigated and it supplies over 40% of the world's food (Droogers et al., 2010). Global warming and the intensification of the hydrological cycle, with the increased occurrence of droughts and floods, will threaten the natural availability of water, enhancing the need of irrigation (Allan and Soden, 2008; Kummu et al., 2016; Rockström et al., 2012; Vörösmarty et al., 2000). The projected population growth will aggravate this already complicated panorama, due to the consequent increase of food demand. The knowledge of irrigated lands and the water used is hence of primary importance to prevent water wastage, to avoid illegal withdrawals and to ensure food and water security (Siebert et al., 2010; Taylor et al., 2013). Monitoring irrigation is also fundamental for other applications: (i) to understand the consequences of irrigation water cycle modifications, (ii) to investigate the impact of irrigation on

local and regional climate conditions, and (iii) to develop hydrological and climate models that account for irrigation (Sacks et al., 2009).

Despite its importance, a global dataset of irrigation water use over long periods is still missing. Available time series of irrigation amount are mostly based on statistical surveys. This kind of information does not take into account the illegal pumping and is potentially affected by large errors, because of self-reporting bias, spatial inconsistency and low temporal resolution and coverage (e.g. the U.S. Geological Survey publishes a report on water use every 5 years) (Deines et al., 2017). Their quality is hence variable over different states and regions as inferred by Siebert et al. (2005) who developed a global dataset of area equipped for irrigation by combining sub-national irrigation statistics. A different approach consists in modeling water requirements for crop irrigation rather than actual water used for irrigation (Doll and Siebert, 2002; Wada et al., 2014), but the existence of vast under and over irrigated areas with respect to water requirements (Foley et al., 2011) represents a large source of errors for this methodology that limits its applicability.

In this context, a new source of irrigation information is emerging, i.e. the use of soil moisture, SM, observations. For decades, SM has been widely used by farmers to efficiently schedule irrigation (Campbell and

Campbell, 1982; Khan et al., 1996; Aguilar et al., 2015). Its knowledge helps to determine the crop stress conditions and then assists the farmer to decide when and how much water must be applied for improving the efficiency and the quality of the production.

Recently, SM has been also employed to directly quantify the amount of water used for irrigation (Brocca et al., 2018; Li et al., 2019; Zaussinger et al., 2019). For instance, Li et al. (2019) used in situ SM data to estimate soil water budget components, including irrigation. The results show that SM potentially can identify irrigation amounts and frequencies. Zaussinger et al. (2019) and Brocca et al. (2018) used remote sensing derived SM data. Zaussinger et al. (2019) developed a methodology to estimate irrigation water use by comparing satellite and modelled SM (which does not include irrigation information), over the Contiguous United States. They validated the estimated irrigation amount against the 2013 Farm and Ranch Irrigation Survey (USDA, 2014). Despite the good results obtained, the validation of the estimated irrigation in different terrains and different climate conditions appears difficult due to the different period of time of the benchmark dataset (they considered the 2013 growing season against the satellite data from 2013 to 2017) and its state-level aggregation.

A different approach to estimate irrigation amount from SM has been developed by Brocca et al. (2018). Through a modified version of SM2RAIN algorithm (Brocca et al., 2014), they demonstrated that two consecutive satellite soil moisture measurements (in addition to ancillary rainfall data) can be used to obtain irrigation estimates at daily time scale. The algorithm is based on an inversion of soil water balance equation to derive the total amount of water entering into the soil. In practice, from SM measurements the irrigation estimation is possible by subtracting the measured rainfall fraction from the total water estimated by the algorithm (which inherently includes irrigation). In Brocca et al. (2018) a preliminary synthetic study, to demonstrate the feasibility of the approach, and a subsequent investigation in nine pilot sites over the world has been performed. Due to the lack of in situ irrigation data, only qualitative assessment was carried out showing relatively good agreement of irrigation estimates by different satellite SM products over regions characterized by long dry periods and in which satellite soil moisture products perform reasonably well. The method has also been tested by using satellite SM data in two sites, respectively in Nebraska and Iran (Brocca et al., 2017; Jalilvand et al., 2019), where irrigation data were available.

The work of Brocca et al. (2018) and Zaussinger et al. (2019) highlighted some important limitations mainly related to low spatial and temporal resolution of current available satellite soil moisture observations. Indeed, most of them have a spatial resolution larger than 20 km, while an irrigated field can range from few thousands of meters to few squared kilometers. As a result, the irrigation signal is usually masked out from the presence of other features contained in the coarse scale satellite pixel. Moreover, a low irrigation signal has a high risk of being indistinguishable from the inherent noise in the satellite derived SM signal (Su et al., 2015; Massari et al., 2017b). The use of higher spatial resolution SM observations as those derived from Synthetic Aperture Radar instruments like Sentinel-1 (Bauer-Marschallinger et al., 2018) could solve this problem for fields with an area similar to the one of the satellite's pixel (in this case 1 km), but their limited temporal resolution (one observation every 1.5–4 days over Europe when the two Sentinel-1 satellites are considered) could be inappropriate to detect irrigation applications occurring in few hours.

In summary, three main issues have limited an objective understanding of whether satellite SM measurements can provide useful information on irrigation estimation, namely, the coarse spatial support of satellite SM observations, their relatively low temporal resolution (with respect to the scales of the irrigation practices) and the absence of a reliable benchmark for testing the validity of the approaches developed so far to estimate irrigation volumes from space.

The purpose of this study is to demonstrate that SM is a valuable source of information for assessing irrigation fluxes and to clarify the effects of spatial and temporal resolution on such estimates. Specifically, this manuscript aims to answer the following two questions:

(1) is SM a reliable source for retrieving irrigation fluxes?
(2) can the proposed approach be used with high spatial and low temporal resolution remote sensing data? Can its accuracy be considered sufficient for estimating irrigation?

To reach the objectives, we applied the method of Brocca et al. (2018) in a controlled irrigated experimental field by using an innovative SM dataset inferred from proximal gamma-ray spectroscopy measurements, characterized by high accuracy, competitive footprint and higher temporal resolution with respect to satellite SM data (De Groot et al., 2009; Bogena et al., 2015; Strati et al., 2018; Baldoncini et al., 2018, 2019). A Proximal Gamma-Ray (PGR) and an agro-meteorological station have been installed in an experimental field located in North Italy for a seven-month period. The ^{40}K gamma signal detected by the PGR spectrometer installed at a few meters above the ground is inversely correlated with soil water content and it is not affected by variations in cosmic radiation and soil chemical composition (Strati et al., 2018). The station is able to sense SM at field scale (Baldoncini et al., 2018), from $\sim 10^3$ to $\sim 10^4$ m^2, and it is therefore in between point and satellite measurements ($\sim 10^8$ m^2), optimal for agricultural application. It is also characterized by high temporal resolution (1 h) hence it is able to track SM variations induced by irrigation.

The paper is organized as follows: Section 2 presents the description of the experimental site and setup; Section 3 synthesizes how SM can be inferred from PGR spectroscopy measurements and the basic principles of the proposed algorithm for irrigation estimation; the results, the discussion and the test at lower temporal resolution are illustrated in Section 4. Lastly, conclusions are drawn in Section 5.

2. Experimental site and setup

The experimental site is a 40 × 108 m^2 tomato test field (44.57° N, 11.53° E; 16 m above sea level) belonging to a research center of the Emiliano-Romagnolo Canal (CER) irrigation district in the Emilia Romagna region, Italy (Fig. 1a). According to the Köppen-Geiger climate classification (Peel et al., 2007), this geographical area is classified as Cfa (temperate climate, without dry season and with hot summer). Emilia Romagna is the Italian region having the largest land surface cultivated with tomatoes, one of the most water-demanding crops among vegetables, and it contributes for about one third of the tomato national production (ISTAT, 2017).

The experimental setup is composed of a Proximal Gamma-Ray, PGR, station equipped with a 1 L NaI(Tl) detector placed at 2.25 m above the ground and a commercial agro-meteorological station (MeteoSense 2.0, Netsens; see Fig. 1a) (Strati et al., 2018). During the data taking period (from 4 April to 2 November 2017), the minimum temperature, T_{min}, ranged from 1.3 °C to 22.7 °C and the maximum temperature, T_{max}, ranged from 13.5 to 39.3 (Fig. 1b); the Short Wave Incoming Radiation (*SWIR*) varied from 34.7 to 257.3 W/m^2 (Fig. 1c). The evapotranspiration (*ET0*, Fig. 1c) is calculated on the basis of the Hargreaves method (Hargreaves and Samani, 1985) by using weather data recorded by the agro-meteorological station.

Tomato plants were transplanted on 23 May with a plant density of 3.5 plants/m^2 and harvested on 14 September. The crop phenological growth stages of anthesis (the time of flowering) and maturity, together with the dates of planting and harvesting, are indicated in Fig. 1b. Irrigation water was delivered by a sprinkler system, according to a schedule provided by the IRRINET decision support tool (Munaretto and Battilani, 2014). The irrigation measurements refer to the water pumped to the sprinkler system. In order to account the losses due to leakage, wind drift, spray droplet evaporation and evaporation from leaf surfaces, a scaling factor of 0.9 is applied to each measurement, as indicated from the field managers.
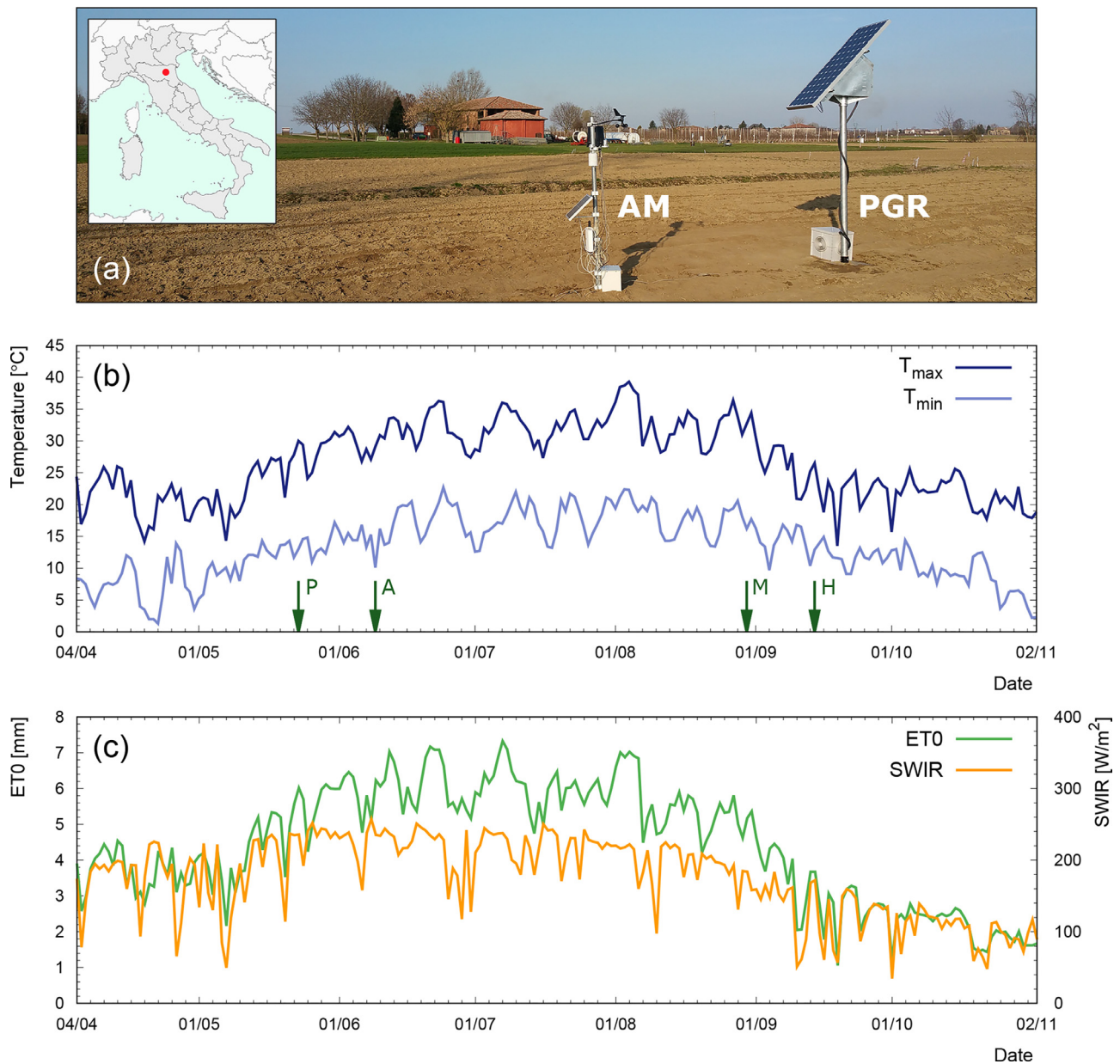
Fig. 1. Panel (a), Proximal Gamma-Ray (PGR) and agro-meteorological (AM) stations, and location of the study area. Panels (b) and (c), weather parameters recorded by the AM station during the data period, i.e. 4th of April–2nd of November 2017: maximum (T_{max}) and minimum (T_{min}) temperature (panel b), Short Wave Incoming Radiation (SWIR) and reference evapotranspiration (ET0) (panel c); ET0 is calculated by using the Hargreaves equation (Hargreaves and Samani, 1985). The arrows in panel (b) indicate the four major crop maturity phases, i.e., planting (P, 23 May), anthesis (A, 9 June), maturity (M, 30 August), and harvesting (H, 14 September).

The soil has a loamy texture characterized by 45% of sand, 40% of silt and 15% of clay; soil bunk density is 1345 kg/m^3 and the organic matter content is 1.26%. The hydraulic properties in terms of wilting point (0.09 m^3/m^3), field capacity (0.32 m^3/m^3), and saturation (0.48 m^3/m^3) were inferred from the water retention curve reported in Strati et al. (2018).

3. Methods

### 3.1. Field scale soil moisture monitoring with gamma-ray spectroscopy

Nuclear non-invasive and non-contact techniques have been developed for filling the gap between punctual ($\sim$m^2) and satellite coarse resolution scale ($\sim 10^5$ m^2) SM data. The Cosmic-Ray Neutron and Proximal Gamma-Ray (PGR) methods demonstrated to effectively probe

SM with a field scale footprint ($\sim 10^4$ m^2) up to a depth of $\sim$ 30 cm, limiting costs and manpower, and using real-time and wireless sensors (Andreasen et al., 2017; Baldoncini et al., 2018; Strati et al., 2018; Zreda et al., 2008). In particular, the PGR method consists in the quantification of SM by measuring gamma signals emitted in the decay of ^{40}K naturally present and typically homogeneously distributed in the agricultural soil.

A gamma-ray spectroscopy measurement is extremely sensitive to different soil water contents as water is much more effective in attenuating gamma rays with respect to minerals typically present in the soil. Indeed, the measured ^{40}K gamma signal $S(t)$ [counts per second] at time t is inversely proportional to the volumetric soil water content SM [m^3/m^3] (Baldoncini et al., 2019; Strati et al., 2018):

$$\text{SM}(t) = \left(\frac{A(t)}{S(t)} - 0.903 \right) \rho \qquad (1)$$
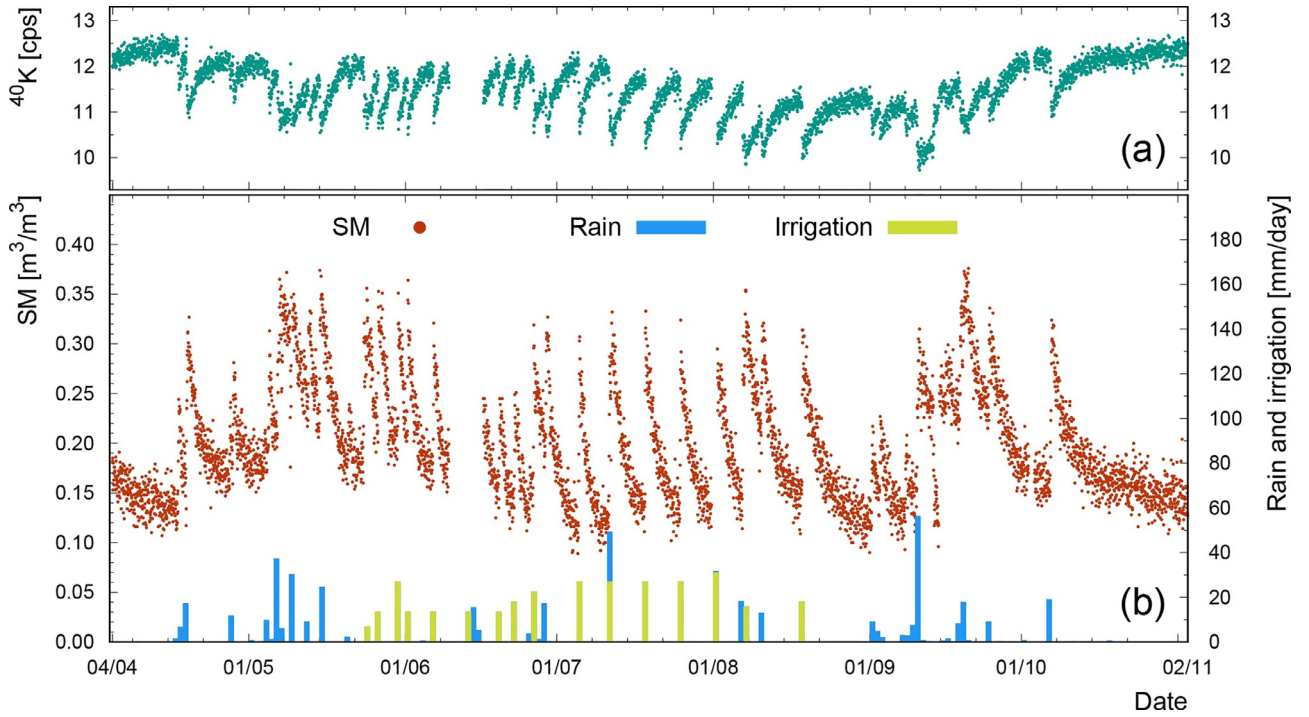
Fig. 2. Panel (a) ^{40}K gamma signal in cps (green points., panel b) volumetric soil water content SM (red points) estimated on the basis of gamma spectroscopy measurements and corrected for the attenuation due to the biomass water content, and daily amount of rainfall (blue lines) and irrigation water (yellow line) are reported for the data taking period (4 April–2 November). ^{40}K gamma signals and SM values are hourly averaged. (For interpretation of the references to color in this figure legend, the reader is referred to the web version of this article.)

with

$$A(t) = S^{Cal} \times \Lambda(t) \times \left[w^{Cal} + 0.903 \right] \qquad (2)$$

where $\Lambda(t)$ is the adimensional time dependent biomass water content correction factor (Baldoncini et al., 2019) and ρ is the soil bulk dry density (kg/m^3). S^{Cal} is the ^{40}K gamma signal recorded at calibration time when the gravimetric soil water content w^{Cal} [kg/kg] was determined on soil samples.

Indeed, the horizontal and vertical horizons of PGR spectroscopy can be defined according to the probability law governing the survival of photons when traversing a material, as in Feng et al. (2009). Given a fixed detector at ~2 m height and a typical 1.3×10^3 kg/m^3 soil density, it can be estimated that 95% of the unscattered gamma photon flux reaching the spectrometer comes from an area with a radius of ~ 25 m (Fig. 2) and from a depth of ~ 30 cm (Fig. 1 of Baldoncini et al., 2018).

3.2. Quantifying irrigation by the inversion of the water balance equation

The idea to invert the soil water balance equation was initially developed to retrieve rainfall from in situ and satellite SM data (Brocca et al., 2015, 2016, 2017; Ciabatta et al., 2017; Koster et al., 2016; Massari et al., 2017a). Here a similar approach is applied, following the work done by Brocca et al. (2018). Specifically, the soil water balance equation for a layer depth Z can be described by the following equation:

$$Z \cdot n \cdot \frac{\mathrm{dSM}(t)}{\mathrm{d}t} = r(t) + i(t) - g(t) - sr(t) - e(t) \qquad (3)$$

where Z [mm] is the soil layer depth, n [m^3/m^3] is the soil porosity, SM(t) [–] is the relative saturation of soil, t [days] is the time, $r(t)$ [mm/days] is the rainfall rate, $i(t)$ [mm/days] is the irrigation rate, $g(t)$ [mm/days] is the drainage (deep percolation plus subsurface runoff) rate, $sr(t)$ [mm/days] is the surface runoff and $e(t)$ [mm/days] is the

actual evapotranspiration. Drainage can be expressed by:

$$g(t) = a \cdot \mathrm{SM}(t)^b \qquad (4)$$

where a [mm/days] and b [–] are two parameters expressing the nonlinearity between drainage rate and SM (Brocca et al., 2014). $sr(t)$ can be considered negligible, since the irrigation through sprinkler system should avoid the formation of surface runoff, if carried out optimally. There is still the possibility that very intense or frequent water application (rainfall or irrigation) could saturate the soil and could lead to surface runoff. The resulting underestimation is a residual error to be accepted, since SM cannot keep trace of the runoff. Finally, actual evapotranspiration is assumed linearly related to reference evapotranspiration:

$$e(t) = \mathrm{ET0} \cdot \mathrm{SM}(t) \qquad (5)$$

Therefore, Eq. (3) can be simplified into:

$$r(t) + i(t) = Z^* \cdot \frac{\mathrm{dSM}(t)}{\mathrm{d}t} + a \cdot \mathrm{SM}(t)^b + \mathrm{ET0} \cdot \mathrm{SM}(t) \qquad (6)$$

where Z^* is $Z \times n$.

One of the main issues associated with this approach is that the direct inversion of Eq. (6) inherently leads to false irrigation estimates if the soil moisture signal is highly noisy. To prevent this problem, a semi-empirical exponential filter (Wagner et al., 1999) was applied to SM data, which depends on a single parameter representing the characteristic time scale of SM variation, T. Once denoised, the SM signal can be used in Eq. (6) to estimate the sum of irrigation and rainfall rate.

The calibration of the three parameters (Z^*, a and b) was carried out by minimizing the Root Mean Square Error (RMSE) between observed and estimated rainfall plus irrigation data. In this perspective, the limited availability of irrigation observation could pose severe limits on the application of the method. Two different calibration procedures were therefore used to test the actual need of irrigation observed data: the
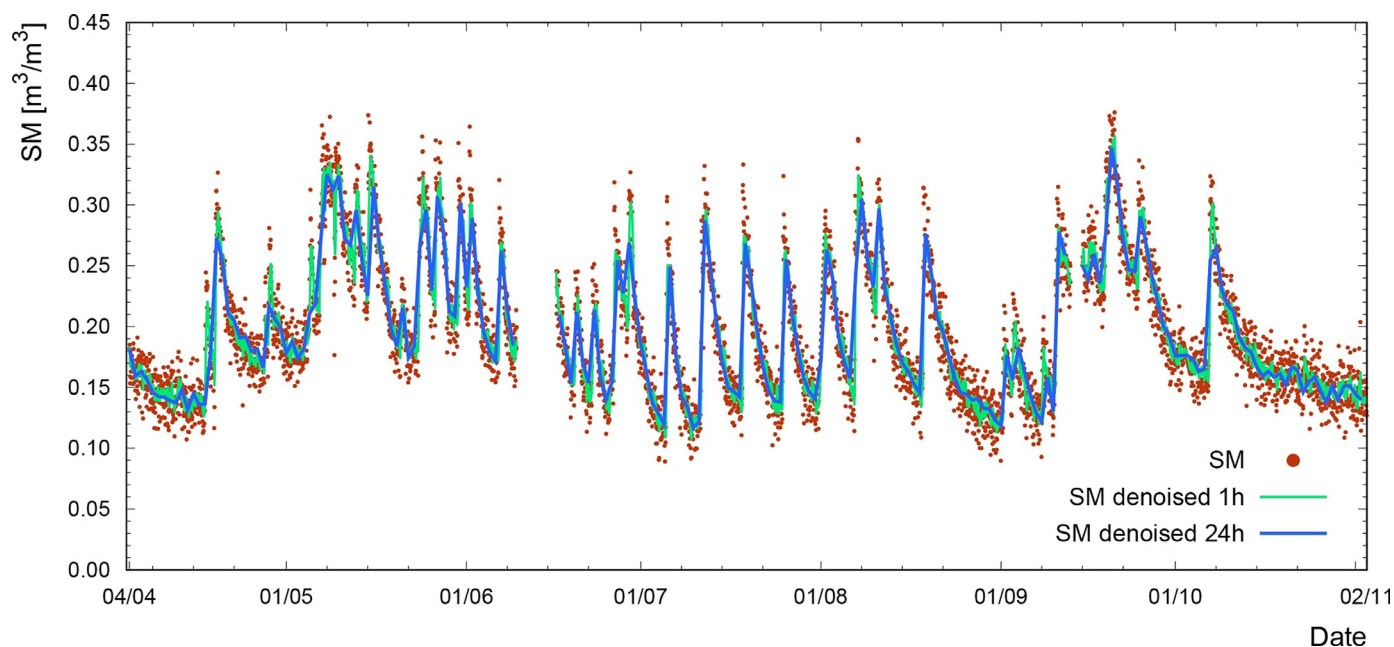
Fig. 3. Denoised PGR SM time series. The hourly raw data (red circle) are first interpolated with a maximum no data gap of 5 h and then filtered with the exponential filter (green line). The resulting data are then sampled each 24 h (blue line). (For interpretation of the references to color in this figure legend, the reader is referred to the web version of this article.)

first calibration (Rain+Irr from here onward) is performed for the entire period using both rainfall and irrigation data, whereas the second one (Rain) is performed by using only rainfall data. For the latter, assuming that no irrigation is applied when rainfall occurs, the calibration is performed only on days where $r(t) \neq 0$. This is a fundamental hypothesis, because during days in which both rainfall and irrigation occur, the algorithm will force the total water infiltrated into the soil at the value of the rainfall only, leading to an underestimation error. The rationale is that if the two calibration procedures provide similar results in terms of irrigation estimation, the method can be confidently applied with no restrictions beside the hypothesis above.

Once the parameters' calibration is performed, the irrigation rate can be calculated by simply subtracting the observed rainfall rate from the outcomes of Eq. (6).

4. Results and discussion

This section describes the estimation of SM from PGR spectra and the estimation of the irrigation through the application of above presented algorithm. Estimated rainfall and irrigation are then compared against true rainfall and irrigation fluxes by using two performances indices: the Pearson Correlation coefficient, *R*, and the Root Mean Square Error, RMSE. Finally, the role of SM data temporal resolution is investigated.

4.1. Soil moisture estimation through proximal gamma-ray spectroscopy

Soil moisture was determined with hourly temporal resolution on the basis of PGR measurements for almost the entire 7 months data-taking period (Fig. 2). The PGR measurement is sensitive to more than half experimental field and therefore well represents the mean soil moisture of the field. The gamma and agro-meteorological stations installed at the tomato experimental field were operative for a 94.8% overlapping duty cycle and a 260 GB global amount of uncompressed data was recorded. As both stations were equipped with a GPRS connection, it was possible to remotely process the data in real time.

PGR ^{40}K signal (Fig. 2a) and SM (Fig. 2b) continuous time series show a strong correlation with rainfall and/or irrigation events, also

in cases of low amounts of distributed water. PGR measurements are indeed able to provide high frequency SM estimations sensitive to transient soil water content levels, consistently with physical-hydrological soil properties. The reliability of the method was tested against validation gravimetric measurements on soil samples, resulting in a ~2% average discrepancy, and against 3 different soil-crop hydrological models (Strati et al., 2018).

Provided a calibration of SM through direct measurements on soil samples and a correction accounting for the biomass shielding effect, PGR spectroscopy performed with a permanent station can be considered an effective non-stop and non-invasive SM monitoring method.

4.2. From soil moisture to irrigation

PGR SM data were processed through the irrigation estimation algorithm to verify the feasibility to estimate rainfall and irrigation amounts from SM. An hourly linear interpolation was applied to estimate SM values during the shutdown periods of the PGR station. If no value was found within a maximum interpolation gap of 5 h, the corresponding SM was excluded from the analysis. The semi-empirical exponential filter was applied to the resulting SM data with 1 h temporal resolution: *T* parameter was fixed at 0.16 days (around 4 h) after the calibration of the algorithm. The denoised SM data were then sampled every 24 h at 00:00 UTC to obtain a daily series of SM used as input of Eq. (6) to predict daily rainfall and irrigation rates. Fig. 3 shows the filtered SM data and the results of the sampling, for the full observation period between April and November 2017. The data between the 13th and the 14th of September were masked out due to the presence of harvesting machines in the field that interfered with the measurements.

Then, the three parameters of the algorithm (Z^*, *a* and *b*) were calibrated through an iterative process, by setting their initial values to the minimum plus 10% of the selected range of variation (Table 1). The outcomes of the algorithm were finally iteratively compared with the observed rainfall plus irrigation rates (Rain+irr calibration) or with the observed rainfall rates (*Rain* calibration) until the *RMSE* is minimized.

The optimized values of the parameters are shown in Table 1, for Rain+Irr and Rain calibration procedures. The Z^* parameter value is par-
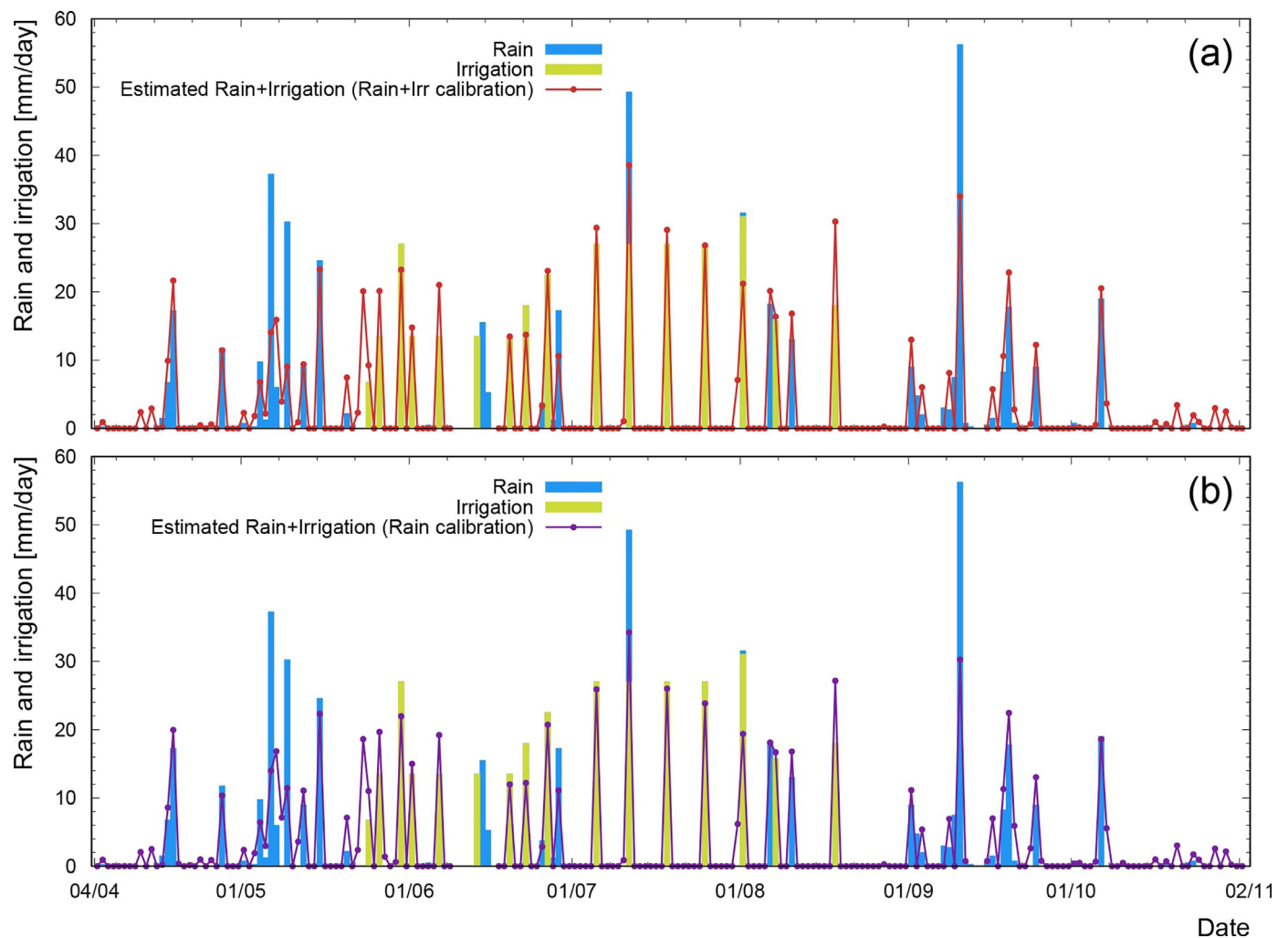
Fig. 4. Rainfall plus Irrigation data derived from Rain+Irr calibration (red line, panel a) and Rain calibration (purple line, panel b) at daily time step. Blue bars represent observed rainfall, yellow bars represent observed irrigation. (For interpretation of the references to color in this figure legend, the reader is referred to the web version of this article.)

Table 1
Calibration parameters (Z^*, a and b) of the irrigation estimation algorithm applied to PGR SM data with rainfall plus irrigation (Rain+Irr) and rainfall (Rain) calibration. Minimum and maximum iteration values are the same for both calibration strategies.

	Iteration value		Output calibration value	
	Minimum	Maximum	Rain+Irr	Rain
Z^* [mm]	20.00	200.00	52.08	45.34
a [mm day^{-1}]	0.00	200.00	10.84	12.24
b [–]	1.00	50.00	6.42	3.49

ticularly significant: the PGR station is able to sense SM until ~300 mm of soil (Fig. 1 of Baldoncini et al., 2018), but the gamma contribution is not uniform with sensing depth. Around 55% of the contribution is derived from the first 50 mm of soil, rising to 70–80% for the first 100 cm of soil. Considering this and an average porosity around 0.4–0.5, we expected a value of Z^* around 50, as it is obtained from the calibration of the algorithm. The variation observed on the parameter values are ascribed to the different calibration period. Indeed, *Rain* calibration performs the parameters estimation only in days when rainfall occurs. Nevertheless, the four parameters maintain the same order of magnitude

and the obtained results present just minor differences. The similarities of the two calibration outcomes are also visible in Figs. 4 and 5, where the rainfall and irrigation time series at daily resolution derived on the basis of the two calibration procedures are shown.

Globally, irrigation and rainfall events are successfully detected by the proposed algorithm, for both calibration procedures. However, the algorithm is not able to well reproduce large rainfall/irrigation events, particularly if the calibration is carried out with rainfall data only.

The irrigation time series are calculated by subtracting the observed rainfall from the algorithm outcomes. This procedure leads to negative values in correspondence with rainfall underestimation, e.g. during the months of May and September. Therefore, those values have been set to zero, since they are not related to the irrigation estimation. For both the calibration procedures, the total amount of rainfall and irrigation together with the two indices, R and RMSE, are calculated to evaluate the performance of the proposed algorithm in the estimation of the irrigation series and the rainfall plus irrigation series with respect to the observed data (see Table 2).

The two datasets show very good performances in both the estimation of rainfall plus irrigation and irrigation with R greater than 0.88 in each case. The RMSE is around 3 mm/day when considering just irrigation series and 4 mm/day when considering rainfall plus irrigation series. In fact, when the irrigation is estimated from rainfall plus

Table 2
Comparison between estimated and observed rainfall plus irrigation and just irrigation in terms of Pearson correlation coefficient, R, and Root Mean Square Error, RMSE. The total Irrigation and Rainfall plus Irrigation amounts for observed and estimated series are also shown.

	Irrigation water			Rainfall plus Irrigation water		
	R[–]	RMSE [mm day^{-1}]	Tot [mm]	R[–]	RMSE [mm day^{-1}]	Tot [mm]
Rain+Irr calibration	0.90	2.71	460.09	0.89	4.00	742.28
Rain calibration	0.88	2.84	462.45	0.88	4.11	742.65
Observed	–	–	314.55	–	–	752.35
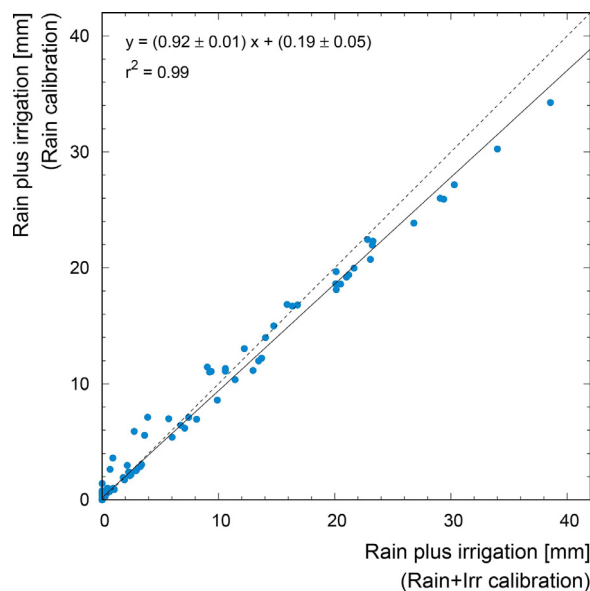
Fig. 5. Scatter plot of rainfall plus irrigation data at daily time step obtained after the application of the algorithm calibrated with Rain+Irr data(x axis) and with just Rain data (y axis). The black dashed line represents the best fit linear curve with slope and intercept parameters respectively equal to (0.87 ± 0.01)[mm/mm] and (0.23 ± 0.06) mm and coefficient of determination $r^2 = 0.99$.

irrigation series, negative values are obtained when rainfall is underestimated. Those values have no physical meanings and are not related to irrigation, therefore they are set to 0. The error component relative to rainfall underestimation is hence eliminated and the overall error decreases. This is also demonstrated by the differences between irrigation and rainfall plus irrigation total error: for each calibration the irrigation amount is always overestimated, whereas the rainfall plus irrigation amount is underestimated. The suppression of the negative impact of rainfall underestimation is responsible of this effect. Finally, the larger underestimation of the outcomes calibrated with just rainfall with respect to the ones calibrated with both rainfall and irrigation is confirmed by the comparison of the two calibrations *RMSE* and total water estimated results. As expected, globally Rain+Irr calibration provides better estimates of irrigation with respect to the *Rain* calibration, because even if the overall overestimation is greater, this is only due to the common rainfall overestimation, i.e. false irrigation events. The first calibration is better in terms of real estimation of irrigation.

Based on the previous analysis, we can answer the first research question. The results show that PGR SM is indeed a reliable information to perform irrigation estimations. The global lack of irrigation information for calibration is not a limit for this methodology, as the decrease of performance when the parameters are calibrated with only rainfall data, is very limited and it can be imputed to the smaller number of calibration data: i.e. the increase of RMSE in estimating rainfall plus irrigation (irrigation) by using *Rain* calibration rather than Rain+Irr calibration

is around 2.75% (4.8%) while the decrease in Pearson correlation is around 0.01 (0.02). Hence, the applicability of this methodology is constrained by the quality of the SM dataset and its spatial and temporal resolution.

4.3. Testing satellite temporal resolution

The application of the proposed algorithm to PGR SM data demonstrated the potential of using SM to derive irrigation. The good results obtained support the use of SM with high spatial resolution. In view of the increased spatial resolution of recent satellite missions for remote SM sensing, it is necessary to test the effect of a lower temporal resolution. Specifically, synthetic SM time series were created by down-sampling PGR SM data at 24, 36, 48, 72 and 120 h in order to reproduce the lower temporal resolution of different remote sensing SM data (e.g., 36 to 144 h for SMOS, SMAP and Sentinel-1). Then, in order to apply the algorithm for irrigation estimation, the series were linearly interpolated at daily scale to obtain daily time series of SM from which daily rainfall and irrigation are computed. As in the previous analysis, the observed rainfall was then subtracted from the algorithm outcomes to obtain irrigation.

A further analysis was carried out by considering the rainfall plus irrigation time series aggregated at 168 h (one week) to average the results in a longer period (i.e., less affected by the interpolation approximations). Indeed, the estimation of irrigation at weekly time scale is still useful for agricultural water management. The performances indices of irrigation series for daily and weekly analysis are shown in Fig. 6.

As expected, the irrigation estimation becomes less accurate as the SM sampling time increases. Nevertheless, the performance drop of daily time series, shown in Fig. 6a and c, is clearly worse than that obtained with weekly time series (Fig. 6b and d). At daily time scale, the interpolated values deviate from the observed values, but this effect can be averaged by analyzing a longer period. Still the tendency of decreasing performance remains, probably due to aliasing problem generated from the sampling procedure, i.e. the missing of some event due to excessive time step. Fig. 6b, in fact, shows that the performance of the weekly product decreases when SM sampling times greater than 48 h are considered. Moreover, the performance for *Rain* calibration is always lower than that for Rain+irr calibration and the discrepancies generally increase with decreasing temporal resolution. The hypothesis in the *Rain* calibration procedure of absence of irrigation when rainfall occurs is probably the main responsible of this behavior.

Based on the previous results, we can answer to the second research question. A temporal resolution lower than one day can be an issue for daily irrigation estimation. Still the outcomes can be acceptable if the temporal resolution is not much greater than 24 h (a Pearson correlation coefficient of around 0.6 was obtained for the products derived from 36 h sampled SM) or if the objective is moved from the estimation of daily to weekly irrigation series. In the latter case, we obtained good results ($R > 0.7$) for SM time sampling up to 48 h. A larger SM sampling time is probably too large to correctly follow the natural variation of SM and the performance indices get worse.
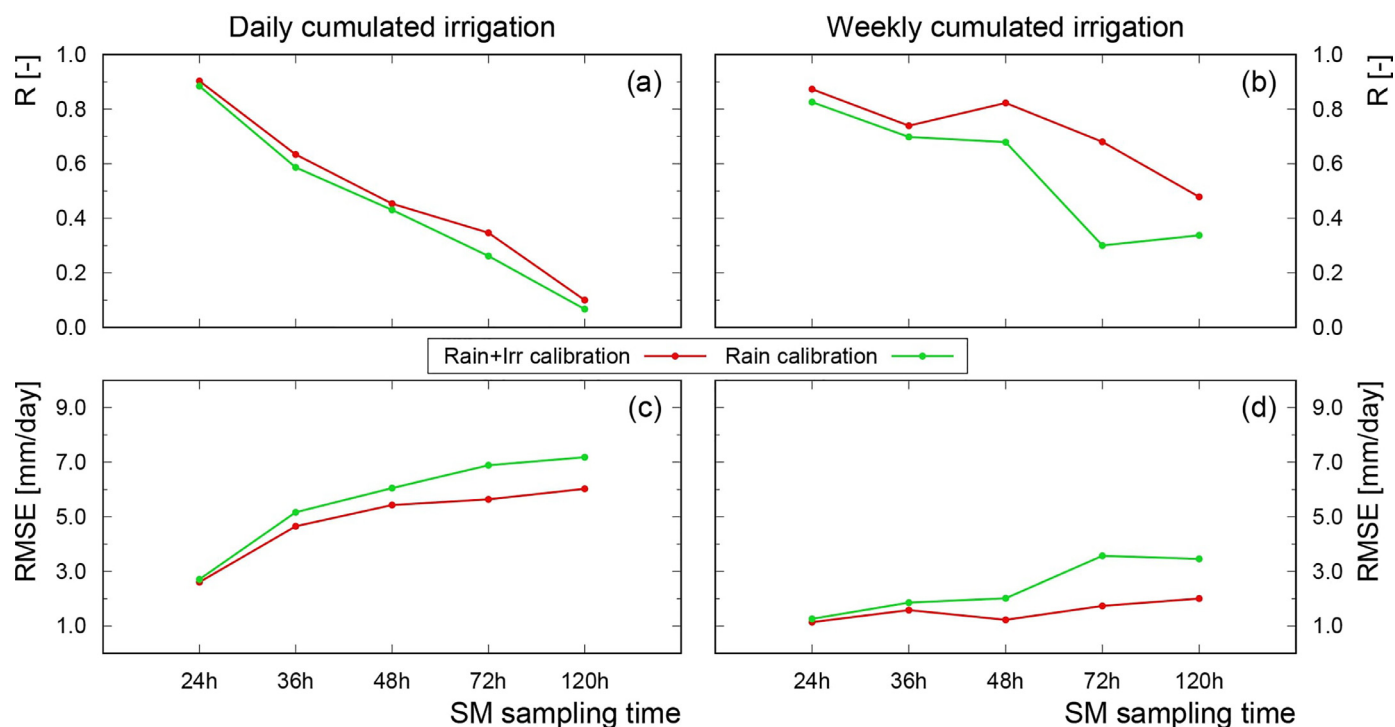
Fig. 6. Comparison between observed and estimated irrigation series derived from SM data at 24, 36, 48, 72 and 120 h temporal resolution, cumulated at 24 h, (a, c) and 168 h (b, d) in terms of Pearson correlation coefficient, *R* (a, b) and Root Mean Square Error, RMSE (c, d). Red and green lines correspond respectively to the results obtained with Rainfall and Irrigation (Rain+Irr) and rainfall (Rain) calibration.

5. Conclusions

In this study SM data inferred from PGR spectroscopy measurements were used as input for a water balance algorithm with the objective to quantify irrigation amount. On the basis of the obtained results, the following conclusions can be drawn.

- PGR spectroscopy proved to be efficient to measure SM at field scale. PGR data with hourly frequency are highly sensitive to transient SM levels and are well correlated with irrigation and rainfall events. Nevertheless, SM data are quite noisy and needed to be filtered.
- The proposed algorithm to estimate irrigation shows good performances with Pearson correlation coefficient between observed and estimated daily irrigation greater than 0.88 both when the algorithm is calibrated with daily rainfall and irrigation data and with just daily rainfall data. In particular, even if the rainfall plus irrigation calibration performs better, the Pearson correlation between observed and estimated irrigation (rainfall plus irrigation) decreases by less than 0.02 (0.01) and the RMSE increases by of 4.8% (2.75%) if the rain calibration is applied, showing that the methodology is applicable also when irrigation data are absent.
- The analysis of data sampled at different time steps, reproducing the lower temporal resolution of high spatial resolution SM remote sensing data, shows that the methodology is potentially applicable also in this case if SM sampling times shorter than 48h are considered. This is the consequence of the drop in performance observed at lower temporal resolution due to daily interpolation problems and aliasing effect. The impact of the interpolation can be partially avoided if an aggregation of the results is carried out at weekly scale.

The analysis enabled to address the two research questions above proposed. In particular:

(1) SM is a reliable source of information for retrieving irrigation amounts and the proposed algorithm is effective in doing so, even

in the case in which only rainfall data are used to calibrate the algorithm.
(2) The algorithm performs relatively well with daily data. A lower temporal resolution can be accepted if the SM sampling time is not greater than 48 h or when the objective is to obtain irrigation estimates on a time scale longer than one day (e.g. on a weekly time scale).

The main purpose of this study was to assess the capabilities of SM to estimate irrigation water and the potential application of the proposed methodology to HR remote sensing data. This would permit to quantify irrigation over large regions (e.g., continental scale) without the need of in situ stations, while accepting a probable decrease in performance due to the lower spatial and temporal resolution, and lower accuracy. Further developments in this direction (e.g. the application of the methodology directly to HR SM remote sensing measurements) are currently being studied and will be the object of future works

Declaration of Competing Interest

None.

Baldoncini, Marco Bittelli, Carlo Bottardi, Enrico Chiarelli, Giovanni Fiorentini, Domenico Solimando for enlightening discussions and valuable comments. The authors thank the University of Ferrara and INFN-Ferrara for the access to the COKA GPU cluster.

References

Aguilar, J., Rogers, D., Kisekka, I., 2015. Irrigation scheduling based on soil moisture sensors and evapotranspiration. Kansas Agric. Exp. Stn. Res. Rep. 1 (5). http://dx.doi.org/10.4148/2378-5977.1087.

Allan, R.P., Soden, B.J., 2008. Atmospheric warming and the amplification of precipitation extremes. Science 321 (5895), 1481–1484. http://dx.doi.org/10.1126/science.1160787.

Andreasen, M., Jensen, K.H., Desilets, D., Franz, T.E., Zreda, M., Bogena, H.R., Looms, M.C., 2017. Status and perspectives on the cosmic-ray neutron method for soil moisture estimation and other environmental science applications. Vadose Zone J. 16 (8). http://dx.doi.org/10.2136/vzj2017.04.0086.

Baldoncini, M., Albèri, M., Bottardi, C., Chiarelli, E., Raptis, K.G.C., Strati, V., Mantovani, F., 2018. Investigating the potentialities of Monte Carlo simulation for assessing soil water content via proximal gamma-ray spectroscopy. J. Environ. Radioact. 192, 105–116. http://dx.doi.org/10.1016/j.jenvrad.2018.06.001.

Baldoncini, M., Albèri, M., Bottardi, C., Chiarelli, E., Raptis, K.G.C., Strati, V., Mantovani, F., 2019. Biomass water content effect in soil water content assessment via proximal gamma-ray spectroscopy. Geoderma 335, 69–77. http://dx.doi.org/10.1016/j.geoderma.2018.08.012.

Bauer-Marschallinger, B., Freeman, V., Cao, S., Paulik, C., Schaufler, S., Stachl, T., Modanesi, S., Massari, C., Ciabatta, L., Brocca, L., Wagner, W., 2018. Toward global soil moisture monitoring with sentinel-1: harnessing assets and overcoming obstacles. IEEE Trans. Geosci. Remote Sens. 99, 1–20. http://dx.doi.org/10.1109/TGRS.2018.2858004.

Bogena, H.R., Huisman, J.A., Güntner, A., Hübner, C., Kusche, J., Jonard, F., Vey, S., Vereecken, H., 2015. Emerging methods for noninvasive sensing of soil moisture dynamics from field to catchment scale: a review. WIREs Water 2 (6), 635–647. https://doi.org/10.1002/wat2.1097.

Brocca, L., Ciabatta, L., Massari, C., Moramarco, T., Hahn, S., Hasenauer, S., Kidd, R., Dorigo, W., Wagner, W., Levizzani, V., 2014. Soil as a natural rain gauge: estimating global rainfall from satellite soil moisture data. J. Geophy. Res. Atmos. 119 (9), 5128–5141. http://dx.doi.org/10.1002/2014JD021489.

Brocca, L., Massari, C., Ciabatta, L., Moramarco, T., Penna, D., Zuecco, G., Pianezzola, L., Borga, M., Matgen, P., Martínez-Fernández, J., 2015. Rainfall estimation from in situ soil moisture observations at several sites in Europe: an evaluation of the SM2RAIN algorithm. J. Hydrol. Hydromech. 63 (3), 201–209. http://dx.doi.org/10.1515/johh-2015-0016.

Brocca, L., Pellarin, T., Crow, W.T., Ciabatta, L., Massari, C., Ryu, D., Su, C.-H., Rudiger, C., Kerr, Y., 2016. Rainfall estimation by inverting SMOS soil moisture estimates: a comparison of different methods over Australia. J. Geophys. Res.-Atmos. 121 (20), 12062–12079. http://dx.doi.org/10.1002/2016JD025382.

Brocca, L., Ciabatta, L., Massari, C., Camici, S., Tarpanelli, A., 2017. Soil moisture for hydrological applications: open questions and new opportunities. Water (Basel) 9 (2), 140. http://dx.doi.org/10.3390/w9020140.

Brocca, L., Tarpanelli, A., Filippucci, P., Dorigo, W., Zaussinger, F., Gruber, A., Fernandez-Prieto, D., 2018. How much water is used for irrigation? A new approach exploiting coarse resolution satellite soil moisture products.. Int. J. App. Earth Observ. Geoinf. 73, 752–766. http://dx.doi.org/10.1016/j.jag.2018.08.023.

Campbell, G.S., Campbell, M.D., 1982. Irrigation scheduling using soil moisture measurements: theory and practice. Adv. Irrig. 1, 25–42. http://dx.doi.org/10.1016/B978-0-12-024301-3.50008-3.

Ciabatta, L., Marra, A.C., Panegrossi, G., Casella, D., Sano, P., Dietrich, S., Massari, C., Brocca, L., 2017. Daily precipitation estimation through different microwave sensors: verification study over Italy. J. Hydrol. 545, 436–450. http://dx.doi.org/10.1016/j.jhydrol.2016.12.057.

De Groot, A.V., Van der Graaf, E.R., De Meijer, R.J., Maučec, M., 2009. Annual irrigation dynamics in the US Northern high plains derived from Landsat satellite data. Geophys. Res. Lett. 44 (18), 9350–9360. http://dx.doi.org/10.1002/2017GL074071.

Deines, J.M., Kendall, A.D., Hyndman, D.W., 2017. Annual irrigation dynamics in the US Northern high plains derived from Landsat satellite data. Geophys. Res. Lett. 44 (18), 9350–9360. http://dx.doi.org/10.1002/2017GL074071.

Doll, P., Siebert, S., 2002. Global modeling of irrigation water requirements. Water Resour. Res. 38 (4) 8–1-8-10 http://dx.doi.org/10.1029/2001WR000355 .

Droogers, P., Immerzeel, W., Lorite, I., 2010. Estimating actual irrigation application by remotely sensed evapotranspiration observations. Agricult. Water Manag. 97 (9), 1351–1359. http://dx.doi.org/10.1016/j.agwat.2010.03.017.

FAO, 2006. AQUASTAT Online Database. Available at: http://www.fao.org/nr/water/aquastat/data/query/index.html.

Foley, J.A., Ramankutty, N., Brauman, K.A., Cassidy, E.S., Gerber, J.S., Johnston, M., Mueller, N.D., O'Connell, C., Ray, D.K., West, P.C., Balzer, C., Bennett, E.M., Carpenter, S.R., Hill, J., Monfreda, C., Polasky, S., Rockström, J., Sheehan, J., Siebert, S., Tilman, D., Zaks, D.P.M., 2011. Solutions for a cultivated planet. Nature 478 (7369), 337. http://dx.doi.org/10.1038/nature10452.

Hargreaves, G.H., Samani, Z.A., 1985. Reference crop evapotranspiration from temperature. Appl. Eng. Agric. 1 (2), 96–99. http://dx.doi.org/10.13031/2013.26773.

ISTAT, 2017. Estimate of areas and production of agricultural cultivations. Available at: http://agri.istat.it/jsp/dawinci.jsp?q=plCPO0000010000023100&an=2017&ig=1&ct=418&id=15A|18A|69A|44A|28A (accessed on 20 February 2018).

Jalilvand, E., Tajrishy, M., Hashemi, S.A.G., Brocca, L., 2019. Quantification of irrigation water using remote sensing of soil moisture in a semi-arid area. Remote Sens. Environ.. in press http://dx.doi.org/10.1016/j.rse.2019.111226 .

Khan, S.R., Rose, R., Haase, D.L., Sabin, T.E., 1996. Soil water stress: its effects on phenology, physiology, and morphology of containerized Douglas-fir seedlings. New Forest 12 (1), 19–39. https://doi.org/10.1007/BF00029980.

Koster, R.D., Brocca, L., Crow, W.T., Burgin, M.S., De Lannoy, G.J.M., 2016. Precipitation estimation using L-band and C-band soil moisture retrievals. Water Resour. Res. 52 (9), 7213–7225. http://dx.doi.org/10.1002/2016WR019024.

Kummu, M., Guillaume, J., de Moel, H., Eisner, S., Flörke, M., Porkka, M., Siebert, S., Veldkamp, T.I.E., Ward, P., J., 2016. The world's road to water scarcity: shortage and stress in the 20th century and pathways towards sustainability. Sci. Rep. 6, 38495. http://dx.doi.org/10.1038/srep38495.

Li, Z., Liu, H., Zhao, W., Yang, Q., Yang, R., Liu, J., 2019. Estimation of evapotranspiration and other soil water budget components in an irrigated agricultural field of a desert oasis, using soil moisture measurements. Hydrol. Earth Syst. Sci. Discus.. https://doi.org/10.5194/hess-2019-89. in review.

Massari, C., Crow, W., Brocca, L., 2017a. An assessment of the performance of global rainfall estimates without ground-based observations. Hydrol. Earth Syst. Sci. 21 (9), 4347–4361. http://dx.doi.org/10.5194/hess-21-4347-2017.

Massari, C., Su, C.H., Brocca, L., Sang, Y.F., Ciabatta, L., Ryu, D., Wagner, W., 2017b. Near real time de-noising of satellite-based soil moisture retrievals: an intercomparison among three different techniques. Remote Sens. Environ. 198, 17–29. http://dx.doi.org/10.1016/j.rse.2017.05.037.

Munaretto, S., Battilani, A., 2014. Irrigation water governance in practice: the case of the Canale Emiliano Romagnolo District, Italy. Water Policy 16 (3), 578–594. http://dx.doi.org/10.2166/wp.2013.092.

Peel, M.C., Finlayson, B.L., McMahon, T.A., 2007. Updated world map of the Köppen-Geiger climate classification. Hydrol. Earth Syst. Sci. 11, 1633–1644. http://dx.doi.org/10.5194/hess-11-1633-2007.

Rockström, J., Falkenmark, M., Lannerstad, M., Karlberg, L., 2012. The planetary water drama: dual task of feeding humanity and curbing climate change. Geophys. Res. Lett. 39 (15). http://dx.doi.org/10.1029/2012GL051688.

Sacks, W.J., Cook, B.I., Buenning, N., Levis, S., Helkowski, J.H., 2009. Effects of global irrigation on the near-surface climate. Clim. Dyn. 33 (2–3), 159–175. http://dx.doi.org/10.1007/s00382-008-0445-z.

Siebert, S., Burke, J., Faures, J.-.M., Frenken, K., Hoogeveen, J., Döll, P., Portmann, F.T., 2010. Groundwater use for irrigation–a global inventory. Hydrol. Earth Syst. Sci. 14 (10), 1863–1880. http://dx.doi.org/10.5194/hess-14-1863-2010.

Siebert, S., Döll, P., Hoogeveen, J., Faures, J.-.M., Frenken, K., Feick, S., 2005. Development and validation of the global map of irrigation areas. Hydrol. Earth Syst. Sci. Discus. 2 (4), 1299–1327. http://dx.doi.org/10.5194/hess-9-535-2005.

Strati, V., Albèri, M., Anconelli, S., Baldoncini, M., Bittelli, M., Bottardi, C., Chiarelli, E., Fabbri, B., Guidi, V., Raptis, K.G.C., Solimando, D., Tomei, F., Villani, G., Mantovani, F., 2018. Modelling soil water content in a tomato field: proximal gamma ray spectroscopy and soil–crop system models. Agriculture 8 (4), 60. http://dx.doi.org/10.3390/agriculture8040060.

Su, C.H., Narsey, S.Y., Gruber, A., Xaver, A., Chung, D., Ryu, D., Wagner, W., 2015. Evaluation of post-retrieval de-noising of active and passive microwave satellite soil moisture. Remote Sens. Environ. 163, 127–139. http://dx.doi.org/10.1016/j.rse.2015.03.010.

Taylor, R.G., Scanlon, B., Döll, P., Rodell, M., Van Beek, R., Wada, Y., Longuevergne, L., Leblanc, M., Famiglietti, J.S., Edmunds, M., Konikow, L., Green, T.R., Chen, J., Taniguchi, M., Bierkens, M.F.P., MacDonald, A., Fan, Y., Maxwell, R.M., Yechieli, Y., Gurdak, J.J., Allen, D.M., Shamsuddha, M., Hiscock, K., Yeh, P.J.F., Holman, I., Treidel, H., 2013. Ground water and climate change. Nat. Clim. Chang. 3 (4), 322. http://dx.doi.org/10.1038/nclimate1744.

USDA., 2014. 2013 Farm and ranch irrigation survey. Available at: https://www.nass.usda.gov/Publications/AgCensus/2012/Online_Resources/Farm_and_Ranch_Irrigation_Survey/fris13.pdf.

Vörösmarty, C.J., Green, P., Salisbury, J., Lammers, R.B., 2000. Global water resources: vulnerability from climate change and population growth. Science 289 (5477), 284–288. http://dx.doi.org/10.1126/science.289.5477.284.

Wada, Y., Wisser, D., Bierkens, M.F.P., 2014. Global modeling of withdrawal, allocation and consumptive use of surface water and groundwater resources. Earth Syst. Dyn. 5 (1), 15–40. http://dx.doi.org/10.5194/esd-5-15-2014.

Wagner, W., Lemoine, G., Rott, H., 1999. A method for estimating soil moisture from ERS scatterometer and soil data. Remote Sens. Environ. 70 (2), 191–207. http://dx.doi.org/10.1016/S0034-4257(99)00036-X.

Zaussinger, F., Dorigo, W., Gruber, A., Tarpanelli, A., Filippucci, P., Brocca, L., 2019. Estimating irrigation water use over the contiguous United States by combining satellite and reanalysis soil moisture data. Hydrol. Earth Syst. Sci. 23 (2), 897–923. http://dx.doi.org/10.5194/hess-23-897-2019.

Zreda, M., Desilets, D., Ferré, T., Scott, R.L., 2008. Measuring soil moisture content non-invasively at intermediate spatial scale using cosmic-ray neutrons. Geophys. Res. Lett. 35 (21). http://dx.doi.org/10.1029/2008GL035655.